Formation of the strain-induced electronic superstructure on the magnetite (111) surface

2003 Europhys. Lett. 63 867

(http://iopscience.iop.org/0295-5075/63/6/867)

EUROPHYSICS LETTERS 15 September 2003

Europhys. Lett., **63** (6), pp. 867–873 (2003)

Formation of the strain-induced electronic superstructure on the magnetite (111) surface

I. V. Shvets, N. Berdunov, G. Mariotto and S. Murphy

SFI Laboratories, Physics Department, Trinity College - Dublin 2, Ireland

(received 25 March 2003; accepted in final form 3 July 2003)

PACS. 72.80.Ga – Transition-metal compounds.
PACS. 68.47.Gh – Oxide surfaces.
PACS. 71.38.-k – Polarons and electron-phonon interactions.

Abstract. – We present direct experimental evidence of the formation of a superstructure on the (111) surface of a magnetite, Fe_3O_4 single crystal. The superstructure, which has a periodicity of 42 A and three-fold symmetry, has been observed by means of STM and LEED. Under the correct conditions of oxygen pressure and sample anneal temperature, the superstructure is reproducibly formed throughout most of the sample surface. Clear atomic resolution within the superstructure has been achieved. The characteristics of the superstructure, including its dependency on the tunnel bias voltage and its atomic-scale periodicity, suggest that it is an electronic effect rather than a mosaic of several iron oxide phases. We explain the results in terms of the formation of giant static polarons, although we notice that other types of electron-lattice instabilities such as charge density wave may offer possible explanations. Polarons with dimensions of many interatomic distances in three-dimensional systems are unlikely to exist but the situation for two- and one-dimensional cases is predicted to be different. We suggest three possible scenarios of instability linking the electron band structure and lattice distortions in magnetite: either resulting from reallocation of Fe^{2+} and Fe^{3+} valence states between octahedral sites or, alternatively, from reallocation between octahedral and tetrahedral sites.

Introduction. – Magnetite (Fe_3O_4) is the oldest known magnetic material and is also the origin of the word magnetism. In some respects it is unique, while in many others it is a typical example of a system illustrating a range of important phenomena in materials science, geology [1], medicine [2] and even extra-terrestrial exploration [3].

Magnetite has the inverse spinel crystal structure, which is based on an f.c.c. lattice of oxygen (O^{2-}) anions, containing mixed valence Fe cations in tetrahedrally and octahedrally coordinated interstices. The unit cell contains 32 anions, 8 cations placed at sites with tetrahedral coordination (so-called A-sites) and 16 cations placed at sites with octahedral coordination (B-sites) (fig. 1). The A-sites are occupied by Fe^{3+} ions and the B-sites are filled with an equal number of Fe^{2+} and Fe^{3+} ions. Magnetite is one of the very few oxides with a relatively high electrical conductivity, $\sim 200\,\Omega^{-1}\mathrm{cm}^{-1}$ at 300 K, due to electron hopping between the B-sites [4]. Magnetite is also a well-known example of a material that undergoes a metal-insulator transition, one of the most important phenomena in solid-state physics. At the Verwey temperature $T_V = 115$–124 K, electrons freeze at the B-sites forming a charge ordered state. The exact arrangement of the Fe^{2+} ions within the lattice below T_V, and the presence of short-range or long-range order is the subject of a continuing debate that has

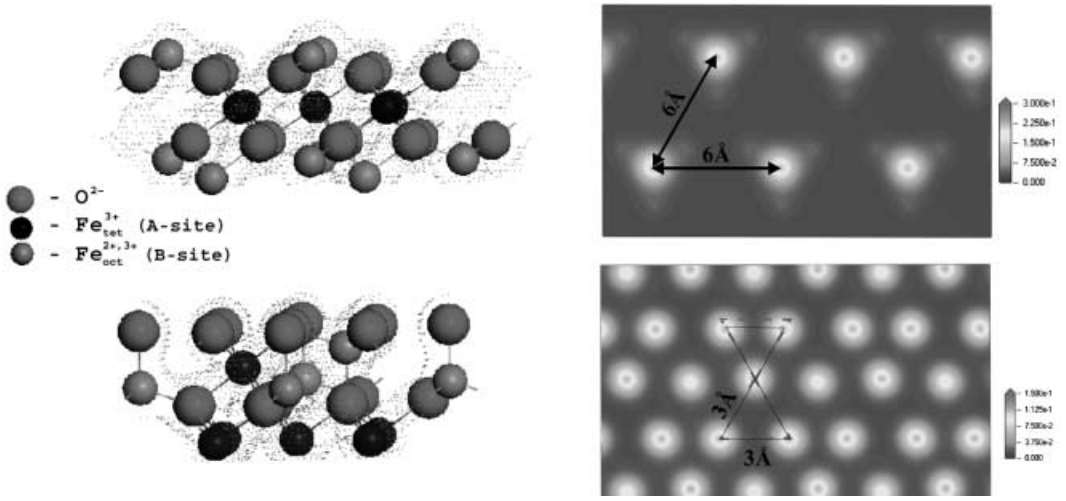

Fig. 1 – Fe_3O_4 (111) crystal structure: Fe-tetrahedral (left-top) termination; oxygen (left-bottom) termination (0.2 level of electron density shown as iso-surface); 2D map of the total charge density (right) above surface calculated for the vacuum slabs shown on the left. Hexagonal symmetry of 3 Å periodic structure is distorted by stress as shown by triangles marking atom displacements.

become more complex as new data becomes available. Despite major efforts aimed at understanding the Verwey transition, even the most general notion that it is caused by the ordering of charges at B-sites is sometimes questioned. It has been suggested that the transition may be caused by bond dimerisation of the electron orbitals [5]. The situation with the metal-insulator transition at the surface is even less understood. Scanning Tunneling Microscopy (STM) studies of the Fe_3O_4 (100) surface have suggested that at 300 K, well above T_V, the charge-frozen state already exists at the surface [6].

It is commonly expected that magnetite has a high spin polarization at the Fermi level. Therefore, it is also a highly interesting material for spin-electronics research. Intuitively, it is clear that in this oxide large-scale superstructures may be formed due to electron-lattice instability as the material includes mobile electrons whose transport is described by lattice-sensitive Hubbard exchange [7]. From private communications we are aware of various attempts to find superstructures in magnetite, *e.g.* by low-angle neutron diffraction. These showed no evidence of superstructure formation in the bulk. The purpose of this study was to establish if long-range electronic superstructures exist in magnetite at the surface and in the subsurface layers. As the electronic structure of the magnetite surface critically depends on its preparation and stoichiometry, it was clear to us at the start of this work that the surface preparation holds the key to the answer.

Experiment. – The sample was grown by the floating-zone technique [8] and cut along the (111) plane with a precision of $\pm 1°$. A characterization of the sample by X-ray powder diffractometry and single-crystal high-resolution diffractometry using a Cu target ($\lambda = 1.54$ Å) showed good agreement with the reference peaks for magnetite. A Verwey transition temperature of 120 K was measured from the discontinuity in the resistivity *vs.* temperature curve, indicating that the crystal is stoichiometric. Measurements of the magnetization of the sample around T_V were performed in fields of 5 to 50 mT, using a vibrating sample magnetometer. The values of T_V obtained from the magnetization and resistivity measurements are consis-

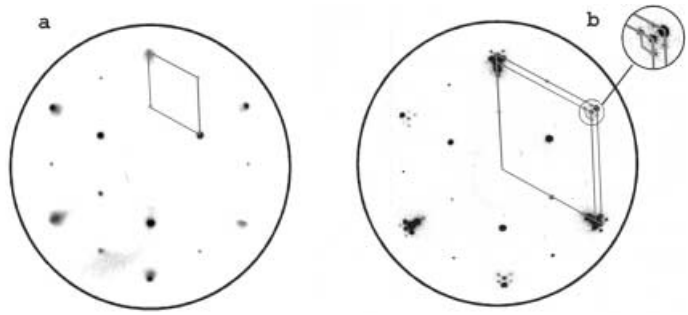

Fig. 2 – LEED patterns of Fe_3O_4 (111) surface at $E = 67\,\text{eV}$. (a) Tetrahedral site Fe termination, $6.0 \pm 0.3\,\text{Å}$ periodicity indicated, and (b) Fe_3O_4 (111) overoxidized surface. Two large rhombs indicate the periodicities of $3.1 \pm 0.1\,\text{Å}$ and $2.8 \pm 0.1\,\text{Å}$; the small rhombus at the highlight shows $42 \pm 3\,\text{Å}$ superstructure.

tent. The value of saturation magnetization of 94 emu/g obtained from the magnetization measurements at 297 K is consistent with the expected value for magnetite. By characterizing the sample using Raman spectroscopy measurements, we were able to positively exclude the presence of other iron oxide phases in the crystal.

The crystal was mechanically polished with diamond paste down to a grain size of $0.05\,\mu\text{m}$, cleaned using organic solvents and transferred into the ultra-high vacuum (UHV) system. Details of our UHV setup are described elsewhere [9]. STM, Auger electron spectroscopy (AES) and low-energy electron diffraction (LEED) measurements were performed at room temperature. Knowing that the electronic structure of the surface is determined by the surface stoichiometry, we have paid a lot of attention to the final steps of the surface preparation in the UHV chamber.

Results and discussion. – We have tried several sample preparation procedures and established two procedures that resulted in the effect reported here. In the first case, the crystal was initially annealed in UHV at a temperature of $950 \pm 15\,\text{K}$ for about 100 hours. It was then ion etched by 2 keV Ar^+ ions (10 min, $I_{\text{target}} = 40\,\mu\text{A}$), annealed in UHV and finally annealed in an oxygen partial pressure of 10^{-6} Torr at $950 \pm 15\,\text{K}$. The oxygen was then removed from the chamber and the crystal was cooled down over 50 minutes in UHV conditions. AES measurements indicated that this method gives rise to a contaminant-free surface. A O(510 eV)/Fe(703 eV) Auger signal ratio of 1.3 was measured. LEED analysis of the surface yielded a p(1 × 1) pattern with a 6 Å periodicity (fig. 2a).

The second preparation differed from the first only in that the crystal was cooled down in an oxygen atmosphere at a pressure of 10^{-6} Torr. It was expected that this procedure led to an increase in the O/Fe ratio [10] on the subsurface layer. This was confirmed by AES spectra taken after the annealing session: the O/Fe ratio increased to 1.45, which, compared to the first sample preparation, indicates an increase of the oxygen in the subsurface. We can note that the O/Fe ratio for the bulk magnetite is expected to be around 1.33. These extra oxygen atoms form an oxygen-terminated surface, where the LEED pattern corresponding to this annealing procedure showed a well-defined hexagonal superlattice with a periodicity of $42 \pm 3\,\text{Å}$ (fig. 2b) without any indication of different iron oxide phases. We could reproducibly toggle between the two surface structures by changing the last step in the preparation. Figure 3a shows a typical STM image obtained after the first preparation procedure. We interpret these results in terms of a surface where the topmost layer consists of Fe^{3+} ions in tetrahedral positions,

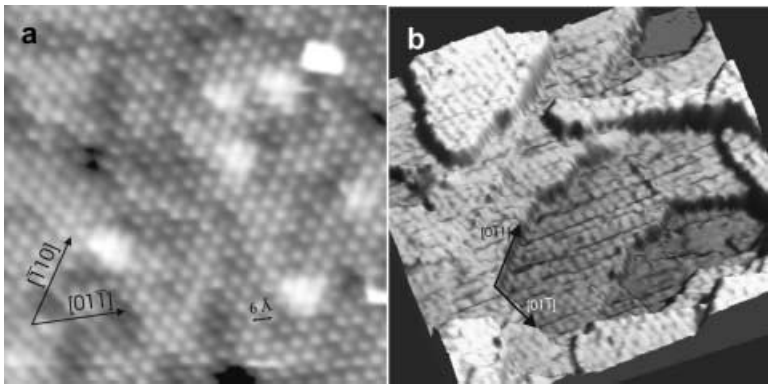

Fig. 3 – (a) $15 \times 15\,\mathrm{nm}^2$ STM image of Fe_3O_4 (111) showing the "regular" type of termination with Fe in tetrahedral sites of 6.0 ± 0.3 Å periodicity. (b) $120 \times 120\,\mathrm{nm}^2$ STM image of overoxidized Fe_3O_4 (111) surface representing large terraces covered by superstructures of about 42 Å period.

forming a hexagonal lattice with a 6 Å periodicity (fig. 1). These results are consistent with the results reported by others on Fe_3O_4 (111) surface [11–13].

Figure 3b shows an STM image of the surface formed after the second preparation procedure. The surface was covered by a superperiodic hexagonal pattern with a 42 Å periodicity, in agreement with the LEED diffraction pattern. This pattern is highly regular and propagates unaltered over a length of over 1000 Å in STM images. Higher-resolution images (fig. 4a) show the arrangement of atoms within this superperiodic structure. One can see that the pattern consists of three distinct areas, marked as areas I, II and III in fig. 4a. Detailed analysis shows that area I has a periodicity of 3.1 ± 0.1 Å, while areas II and III have a periodicity of 2.8 ± 0.1 Å along the [011] direction. The atomic arrangements in areas II and III have exactly the same symmetry and periodicity. The height difference between these areas is bias dependent and varies from 0.6 Å to 0.4 Å as the bias voltage changes from −1.0 V to −0.5 V. The shape of areas II and III also changes with the bias voltage, as illustrated in fig. 4b. We therefore conclude that the observed height difference between area II and III is due to an electronic effect, rather than a topographic one.

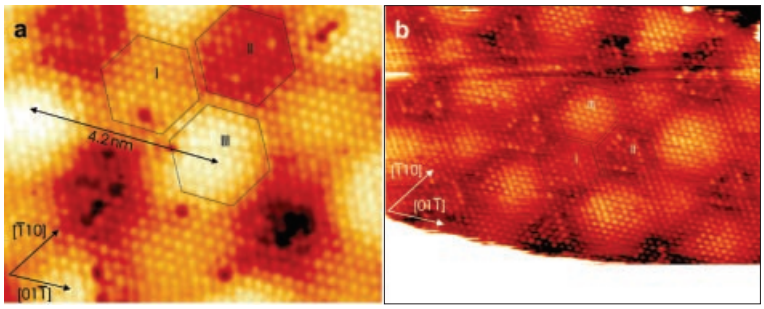

Fig. 4 – (a) $10 \times 8\,\mathrm{nm}^2$ STM image of the superperiodic pattern seen in fig. 3b. Areas II, III have 3.1 ± 0.1 Å interatomic periodicity, and area I has 2.8 ± 0.1 Å periodicity ($V_{\mathrm{bias}} = -1.0$ V). (b) $15 \times 10\,\mathrm{nm}^2$ STM image of the same sample as in (a), with different bias: $V_{\mathrm{bias}} = -0.5$ V. The height difference between areas II and III now is 0.4 Å, instead of 0.6 Å as in (a).

To validate the obtained STM data, we performed Density Functional Theory (DFT) calculations for the structure of the (111) surface of magnetite. The CASTEP algorithm within the local density approximation of DFT [14] was used to calculate total energies and optimize the surface geometry. In fig. 1 we present the total charge density distribution in the Fe-tetrahedral and oxygen termination of bulk magnetite. The maximum of charge density above the surface corresponds to Fe-sites for the Fe-tetrahedral termination, and O-sites in case of the oxygen termination. This is in good agreement with our STM results. We were not able to find a reconstructed surface supersymmetry similar to that observed in the STM images (fig. 4). Nevertheless, shifted positions of oxygen atoms (fig. 1, right-bottom) clearly indicate the stress in the top surface layer that might create a new long-range order.

Superperiodic features have been observed for thin oxide films grown on Pt(111) [12], and also for reduced single crystals of Fe_3O_4 (111) [15]. This results from ordering between multiple phases (FeO, Fe_3O_4 and α-Fe_2O_3). These models cannot be applied to explain our results; the observed $\sim 10\%$ difference in periodicity between area I and areas II, III is significantly greater than the difference in lattice constant between the various oxide phases. Besides, the focus of our attention is the difference between areas II and III that have completely identical atomic structures. It must be noted that the sample preparation routine in [14] differs from ours significantly (reduction *vs.* oxidization) and, in the other case [12], the sample was a thin film. It is well accepted that the surface of an iron oxide critically depends on the details of the preparation routine.

We propose the following explanation for the observed structure. The surface termination with a 3 Å periodicity represents two possible types of closed oxygen layer termination located either above a layer of A-site Fe^{3+} cations, or an Fe-multilayer with a mixture of A- and B-site cations. The DFT calculations performed for both types of oxygen terminations show the local charge density maxima above the oxygen sites. While we could readily image the Fe-terminated surface with a 6 Å periodicity at both negative and positive bias (fig. 3a), atomic resolution on the oxidized surface could only be achieved at a negative bias in the range from -1.0 to -0.5 V (fig. 4a-b). Our conclusion that an O-terminated surface is observed in STM images (fig. 4) is also corroborated by Weiss's *et al.* [12] explanation of experimental results as a Fe_3O_4 (111) surface composed of a topmost layer of oxygen. Dangling bonds at the surface result in excess of electrons that are retained in the topmost oxygen layer. The resulting Coulomb repulsion established between the oxygen anions produces an increase in inter-ion separation from 2.8 Å to 3.1 Å. This translates into tensile stress transferred into the few subsurface layers and modulated along the surface.

The stress through electron-lattice interaction triggers formation of the regular pattern of areas II and III. One could possibly consider such an electron-lattice instability as a giant static polaron [16]. A polaron results from the interaction of electrons with a lattice deformation. A large polaron is defined as polaron with a radius r_p much larger than the lattice constant a. In the classical case of the continuum effective mass approximation for the electron, the polaron radius is

$$r_\mathrm{p} \approx \frac{1.5\hbar k}{me^2}\,, \tag{1}$$

where m and e are the electron mass and charge. $1/k = 1/\varepsilon - 1/\varepsilon_0$, where ε_0 and ε are the dielectric constants with and without distortion caused by interaction of electrons with the lattice. If we take the trial wave function representing a polaron [15],

$$\varphi_\mathrm{p} = \frac{1}{\sqrt{\pi r^3}} \exp\left[-\frac{r}{r_\mathrm{p}}\right], \tag{2}$$

the following formula for the distortion energy associated with the lattice polarization is obtained:

$$E_{\mathrm{d}} = 0.2\alpha_{\mathrm{p}}^2\hbar\omega, \tag{3}$$

where α_{p} is the polaron coupling constant

$$\alpha_{\mathrm{p}} = \frac{e^2}{k\hbar^{3/2}}\sqrt{\frac{m}{2\omega}} \tag{4}$$

and ω is the optical phonon frequency. From the above condition $r_{\mathrm{p}} \gg \alpha_{\mathrm{p}}$ and also from (1) and (4) we can obtain the condition that $\alpha_{\mathrm{p}} \ll 1$. On the other hand, one can show that

$$\alpha_{\mathrm{p}} = \sqrt{\frac{E_{\mathrm{d}}}{0.2\hbar\omega}}\,. \tag{5}$$

The second condition that must be fulfilled to complete the consistent continuum classical approximation is that $\alpha_{\mathrm{p}}^2 \gg 5$, meaning that several phonons are involved in the formation of a single polaron. These two contradictory requirements for α_{p} mean that a large polaron is difficult to realize in practice, and Alexandrov and Mott [15] note that it has not been observed in any known system. On the other hand, the situation in low-dimensional systems could be rather different and polarons could be more stable. It should be kept in mind that the formulas (1)-(5) refer to the case of a gas of weakly interacting carriers. One should be careful in drawing conclusions from these formulas in the case of a magnetic oxide where the electron-phonon interaction is very large and the number of carriers is comparable to the number of sites.

Finally, it could be possible to consider the pattern of areas II and III as a Charge Density Wave (CDW). CDW is also an electronically induced lattice instability accompanied by a modulation of the electronic density. In the case of one-dimensional systems, CDW is known to occur at a wave vector $q = 2k_{\mathrm{F}}$ and is known as Peierls instability. In the case of 2D and 3D systems, a CDW can develop for Fermi liquids with a nested Fermi surface. It is interesting to note that the simulation of the bias voltage dependencies of the STM image of a CDW make good comparison with our bias dependencies (figs. 4a and b) [17]. It is also interesting to note that in our case the corrugation decreases, as the tip gets closer to the surface, because of the bias reduction. This is an unusual behavior for atomic corrugation imaged with STM and yet a typical feature of the CDW image [18].

The surface of magnetite could be particularly susceptible to modulation of the electronic structure due to the presence of Fe^{2+} and Fe^{3+} ions at the B-sites. The strain could cause re-allocation of charges between the octahedral B-sites. There are two possibilities for such re-allocation. According to the first scenario, area III is the area where electrons can move between B-sites as is believed to happen in magnetite at room temperature. In area II, electrons freeze and can no longer hop between the B-sites as in magnetite below T_{V}. In other words, at room temperature area II remains below T_{V} and area III is above T_{V}. Charge freezing at room temperature at the surface of magnetite was proposed by *Weisendanger et al.* [7] although the details of this experiment are completely different. The second scenario is that in area II, all the B-sites are occupied by the Fe^{2+} ions and in area III, by Fe^{3+} ions. We suggest that the second scenario is unlikely, as creation of domains with net charges would be too costly in terms of the Coulomb energy. Although the B-sites are located 0.6 Å below the surface, it is well known that STM images could be affected by subsurface transformations [19].

Another possible reallocation involves the A-sites. For example, area III is the normal conducting magnetite-like state of inverted spinel having Fe^{3+} ions at the A-sites and area II

is in an insulating state of noninverted spinel having Fe^{2+} ions at the A-sites that does not exist in the bulk.

One could formulate the question: is the transition between the states with and without long-range order on magnetite (111) driven by an electron-lattice instability, of the first or the second order? Further experimental evidence is required to address this issue.

Conclusion. – We present here direct experimental evidence of the formation of a superstructure on the (111) surface of a magnetite (Fe_3O_4) single crystal. The characteristics of the superstructure suggest that it is an electronic effect rather than a mosaic of several iron oxide phases. We explain the results in terms of the formation of a giant static polaron although other types of electron-lattice instability such as the charge density wave may offer an explanation. We suggest three possible scenarios of the instability linking the electron band structure and lattice distortions in magnetite: either resulting from reallocation of Fe^{2+} and Fe^{3+} valence states between octahedral sites or, alternatively, from reallocation between octahedral and tetrahedral sites.

* * *

This work was supported by the Science Foundation of Ireland under contract 00/PI.1/C042.

REFERENCES

[1] Schlinden V. and Meyer U., *J. Geophys. Res.*, **104** (1999) 7527.
[2] Jordan A., Scholtz R., Wust P., Fahling H., Krause J., Wlodarczyk W., Sander B., Vogl T. and Felix R., *Intl. J. Hyperthermia*, **13** (1997) 587.
[3] Pettengill A. H. and Simpson R. A., *Science*, **272** (1996) 1628.
[4] Cox P. A., *Transition Metal Oxides. An Introduction to Their Electronic Structure and Properties* (Clarendon Press, Oxford) 1995.
[5] Seo H., Ogata M. and Fukuyama H., *Phys. Rev. B*, **65** (2002) 85107.
[6] Wiesendanger R., Shvets I. V., Buergler D., Tarrach G., Guentherodt H. J., Coey M. and Graeser S., *Science*, **255** (1992) 583.
[7] Mott N. F., in *Metal-Insulator Transitions*, 2nd edition (Taylor and Francis, London) 1990, p. 217.
[8] Koltun R., Herrmann M., Guentherodt V. and Brabers V. A. M., *Appl. Phys. A*, **73** (2001) 49.
[9] Mariotto G., D'Angelo M. D. and Shvets I. V., *Rev. Sci. Instrum.*, **70** (1999) 3651.
[10] Mariotto G., Murphy S. and Shvets I. V., *Phys. Rev. B*, **66** (2002) 245426.
[11] Ketteler G., Weiss W., Ranke W. and Schlögl R., *Phys. Chem. Chem. Phys.*, **3** (2001) 1114.
[12] Weiss W. and Ritter M., *Phys. Rev. B*, **59** (1999) 5201.
[13] Shaikhutdinov Sh. K., Ritter M., Wang X.-G., Over H. and Weiss W., *Phys. Rev. B*, **60** (1991) 11062.
[14] Segall M. D., Lindan P. J. D., Probert M. J., Pickard C. J., Hasnip P. J., Clark S. J. and Payne M. C., *J. Phys. Condens. Matter*, **14** (2002) 2717.
[15] Condon N. G., Leibsle F. M., Parker T., Lennie A. R., Vaughan D. J. and Thornton G., *Phys. Rev. B*, **55** (1997) 15885.
[16] Alexandrov A. S. and Mott N., *Polarons and Bipolarons* (World Scientific Publ.) 1995.
[17] Tersoff J., *Phys. Rev. Lett.*, **57** (1986) 440.
[18] Sacks W., Roditchev D. and Klein J., *Phys. Rev. B*, **57** (1998) 13118.
[19] Osing J. and Shvets I. V., *Surf. Sci.*, **417** (1998) 145.